FEBS Letters 582 (2008) 597–602

The three-dimensional structure of the analgesic α-conotoxin, RgIA

Richard J. Clark[a], Norelle L. Daly[a], Reena Halai[a], Simon T. Nevin[b], David J. Adams[b], David J. Craik[a,*]

[a] *Institute for Molecular Bioscience, The University of Queensland, Brisbane, Queensland 4072, Australia*
[b] *School of Biomedical Sciences, The University of Queensland, Brisbane, Queensland 4072, Australia*

Received 10 January 2008; accepted 17 January 2008

Available online 31 January 2008

Edited by Christian Griesinger

Abstract **The α-conotoxin RgIA is a selective antagonist of the α9α10 nicotinic acetylcholine receptor and has been shown to be a potent analgesic and reduces nerve injury associated inflammation. RgIA was chemically synthesized and found to fold into two disulfide isomers, globular and ribbon. The native globular isomer inhibited ACh-evoked currents reversibly in oocytes expressing rat α9α10 nAChRs but the ribbon isomer was inactive. We determined the three-dimensional structure of RgIA using NMR methods to assist in elucidating the molecular role of RgIA in analgesia and inflammation.**

Keywords: Conotoxin; Nuclear magnetic resonance; Analgesic; Oxidative folding; Disulfide isomers

1. Introduction

Conotoxins are disulfide rich peptides from the venom of marine snails of the *Conus* genus [1]. They are potent and selective ligands for a range of ion channels and have considerable therapeutic potential especially as analgesics [2,3]. The α-conotoxins (Fig. 1) specifically target muscle and neuronal nicotinic acetylcholine receptors (nAChRs) with high potency and selectivity [4]. They range in size from 12 to 19 amino acids, contain two disulfide bonds in a I–III, II–IV topology and have a three-dimensional structure dominated by an α-helix believed to be the scaffold that presents the amino acid side chains in the correct orientation for receptor binding [5].

α-Conotoxins, RgIA [6] and Vc1.1 [7] have potent analgesic activity in rat models of neuropathic pain [8,9]. Both of these conotoxins are specific antagonists of the α9α10 subtype of the nAChR and it was originally proposed that blocking this subtype produced analgesia [9]. However, it has been recently proposed that the α9α10 nAChR is not the analgesic target for these conotoxins as several modified analogues of Vc1.1 are still equipotent at the α9α10 nAChR but have no analgesic activity [10]. The α-conotoxins can be further classified based on the spacing between cysteines II and III and cysteines III and IV. Interestingly, Vc1.1 and RgIA belong to different classes of α-conotoxins, 4/7 and 4/3, respectively, yet they target the same receptor subtype. Determination of the 3D structure of RgIA may yield insights into the factors that make RgIA specific for the α9α10 nAChR subtype. Because of their small size and well-defined structures, conotoxins are ideally suited to structural determination using nuclear magnetic resonance [11].

This study describes the synthesis, oxidative folding and structural elucidation by NMR of the α-conotoxin RgIA. Detailed structural analysis of RgIA will provide a basis for establishing structure/function relationships and may facilitate structure-based design studies to produce more potent and selective analgesic molecules.

2. Materials and methods

2.1. Peptide synthesis

RgIA was assembled by solid-phase peptide synthesis using the in situ neutralization/HBTU protocol for Boc chemistry [12]. The crude peptide was purified by RP-HPLC and characterized by RP-HPLC and ES-MS. The peptide was oxidized in 0.1 M NH_4HCO_3 (pH 8.2) at room temperature. An alternative oxidation buffer of 25% propan-2-ol in 0.1 M NH_4HCO_3 (pH 8.2) was also used that favoured the more hydrophobic globular RgIA disulfide isomer. The oxidized peptide was purified by RP-HPLC. The disulfide connectivity of the two isomers was confirmed using a partial reduction/alkylation strategy with subsequent MS/MS sequencing as described previously [13].

2.2. Electrophysiology

RNA preparation, oocyte preparation and expression of nAChR subunits in *Xenopus* oocytes were performed as described previously [13]. Plasmids with cDNA encoding the rat α9 and α10 nAChR subunits were kindly provided by Dr. A.B. Elgoyhen (Universidad de Buenos Aires, Argentina). Oocytes were injected with 5 ng of cRNA and kept at 18 °C in ND96 buffer (96 mM NaCl, 2 mM KCl, 1.8 mM $CaCl_2$, 1 mM $MgCl_2$ and 5 mM HEPES at pH 7.4) supplemented with 50 mg/l gentamycin and 5 mM pyruvic acid 2–5 days before recording. All recordings were conducted at 20–23 °C using a bath solution of ND96 as described above. During recordings, the oocytes were superfused continuously at a rate of 1.5 ml/min, with 300 s incubation times for the conotoxin. Acetylcholine (ACh; 100 μM) was applied for 2 s at 5 ml/min, with 300 s washout periods between applications. RgIA was co-applied with the agonist. Cells were voltage clamped at a holding potential of −80 mV. Data were sampled at 500 Hz and filtered at 200 Hz. Peak current amplitude was measured before and following incubation of the peptide. All data were pooled (n = 3–9 for each data point) and represent as arithmetic means ± S.E.M., Hill equation was used to fit concentration–response curves using SigmaPlot 8.0 (Jandel Corporation, San Rafael, CA).

2.3. NMR spectroscopy and structure calculations

NMR data for RgIA were recorded on a sample in 90% H_2O/10% D_2O at pH 3.5 using a Bruker ARX 600 MHz spectrometer. 2D NMR experiments included DQF-COSY, E-COSY, TOCSY and NOESY, with all spectra recorded at 280–290 K. A series of 1D and TOCSY spectra acquired immediately following the dissolution of

*Corresponding author. Fax: +61 7 3346 2029.
E-mail address: d.craik@imb.uq.edu.au (D.J. Craik).

0014-5793/$34.00
doi:10.1016/j.febslet.2008.01.027

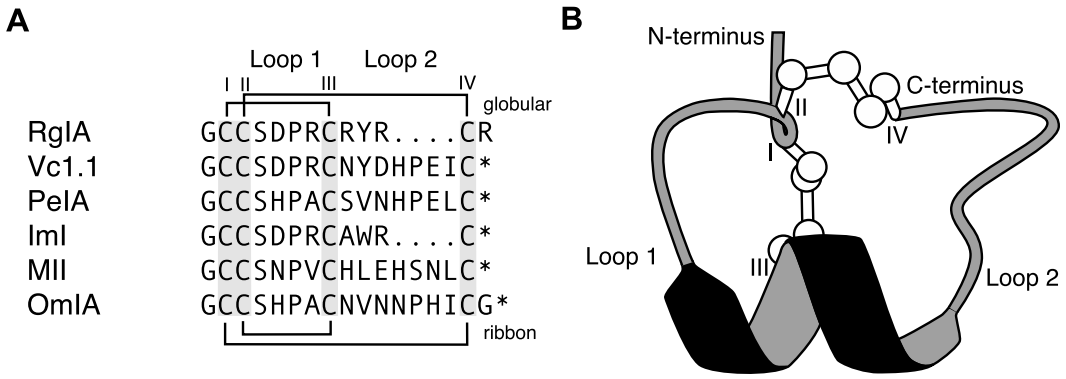

Fig. 1. The α-conotoxins. (A) Selected α-conotoxin sequences showing the cystine frameworks of the globular and ribbon disulfide isomers and the two loops used to define the subclasses of α-conotoxins. The asterisk indicates an amidated C-terminus. (B) Conserved structural scaffold of the α-conotoxins, consisting of two disulfide bonds in a I–III, II–IV arrangement and a central helical region.

fully protonated RgIA in D_2O were used to determine the slow-exchanging NH protons. Peak intensities from a NOESY spectrum with a mixing time of 300 ms at 290 K were used to determine distance restraints. Backbone dihedral restraints were determined from $^3J_{HN-H\alpha}$ coupling constants and ϕ angles were restrained to $-60 \pm 30°$ for $^3J_{HN-H\alpha} < 5.8$ Hz. Intra-residue NOE and $^3J_{H\alpha-H\beta}$ coupling patterns were used in assigning χ^1 angle restraints of some side chains. Two restraints were included for a hydrogen bond identified from D_2O exchange data and preliminary structures.

Initial structures were generated using Cyana software [14] and the final structure calculations were performed using a simulated annealing protocol with CNS [15] as previously described [13]. Fifty structures were calculated and the 20 with the lowest overall energies were retained for analysis (see Table 1). Structures were visualized using MOLMOL [16] and analysed with PROMOTIF [17] and PROCHECK_NMR [18].

Table 1
NMR and refinement statistics for RgIA

NMR distance and dihedral constraints	
Total NOE	55
Sequential ($\|i-j\|=1$)	30
Medium-range ($\|i-j\|<4$)	18
Long-range ($\|i-j>5$)	4
ϕ Restraints	6
Structure statistics	
Violations (mean and S.D.)	
Distance constraints (Å)	0.04 ± 0.007
Dihedral angle constraints (°)	0.28 ± 0.32
Maximum dihedral angle violation (°)	3
Maximum distance constraint violation (Å)	0.3
Deviations from idealized geometry	
Bond lengths (Å)	0.004 ± 0.0002
Bond angles (°)	0.55 ± 0.06
Impropers (°)	0.44 ± 0.09
Average pairwise r.m.s.d.[a] (Å)	
Backbone atoms (residues 2–11)	0.46 ± 0.15
Heavy atoms (residues 2–11)	1.73 ± 0.35
Ramachandran statistics	
Percentage of residues in most favoured region	77
Percentage of residues in additionally allowed region	23

[a]Pairwise r.m.s.d. was calculated among 20 refined structures.

3. Results

The conotoxin RgIA was successfully assembled by solid phase peptide synthesis and the disulfide bonds were formed using a direct oxidative folding approach in aqueous buffer at basic pH. Using NH_4HCO_3 buffer alone resulted in the formation of two disulfide isomers in an approximately 1:1 ratio as shown in Fig. 2. The disulfide connectivity of these two isomers was determined to be the native globular isomer (Cys2-Cys8, Cys3-12) and the non-native ribbon isomer (Cys2-Cys12, Cys3-Cys8). Addition of 25% propan-2-ol to the folding buffer resulted in a greater proportion of the globular isomer being formed as this isomer is more hydrophobic, as reflected in its later elution time on RP-HPLC (Fig. 2B). Addition of a hydrophobic co-solvent is often used to promote formation of the native disulfide isomer when folding conotoxins using a direct oxidation approach. For example, formation of the globular isomer of ImI, which is a member of the same 4/3 sub-class of α-conotoxins as RgIA, is promoted by the addition of methanol, ethanol or propan-2-ol to the folding buffer [19].

NMR data were recorded at 280 K for both isomers; the spectra were assigned and chemical shift analysis indicated that the globular isomer was structurally more similar to the related conotoxin ImI than the ribbon isomer (Fig. 3A). The globular isomer also showed a series of negative secondary shift values for residues 6–9, which is indicative of helical character and consistent with the conserved α-conotoxin framework [4]. In parallel, the effect of each isomer on ACh-evoked currents in *Xenopus* oocytes expressing the rat α9α10 nAChR subtype was investigated (Fig. 2). The globular isomer inhibited the ACh (100 μM)-evoked current reversibly with an IC_{50} of 22 nM (Hill coefficient = 0.9) but the ribbon isomer exhibited no inhibition at concentrations up to 1 μM. On the basis of the preliminary NMR and biological activity data, a three-dimensional structure of the native/globular and active isomer of RgIA was determined. The ribbon isomer was not structurally characterized as it was inactive at the α9α10 nAChR.

The NMR spectra recorded on RgIA showed single spin systems for each residue of the peptide. Several residues including Asp^5, Tyr^{10} and Cys^{12} have broadened resonances, which indicates that there may be some localized conformational exchange. Despite this broadening, there were sufficient NOEs to calculate a 3D structure using a simulated annealing protocol in CNS. A set of 50 structures was calculated with 55 distance restraints consisting of three intra-residue, 30 sequential, 18 medium range and four long range restraints. Six ϕ angle restraints were included and two χ_1 angle restraints. Two restraints for one hydrogen bond between Cys^8 HN and Asp^5

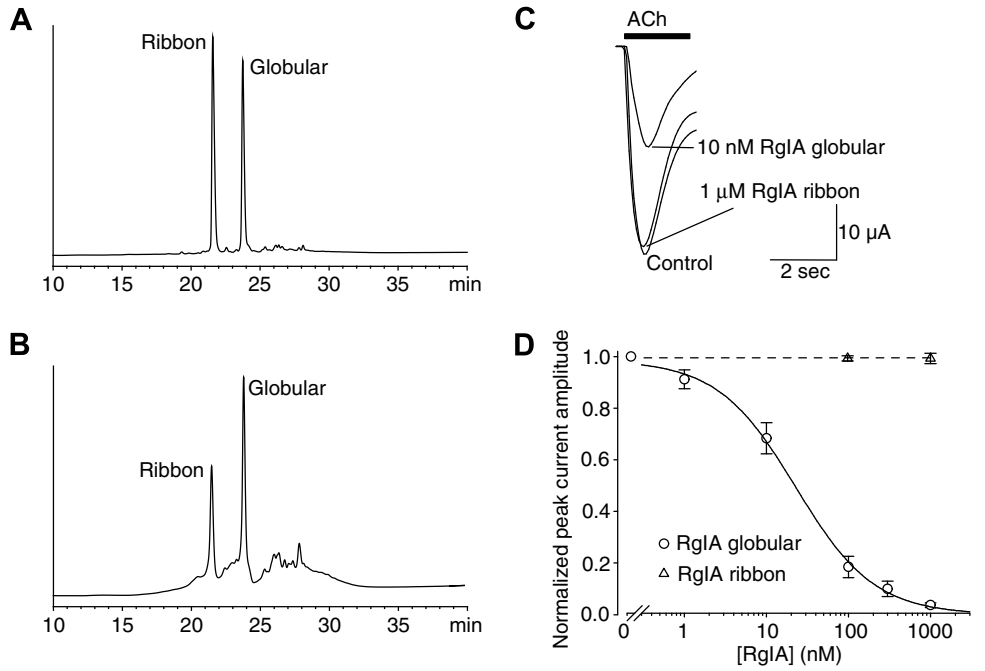

Fig. 2. Oxidative folding and biological activity of RgIA. (A) RP-HPLC oxidation profile of RgIA using 0.1 M NH_4HCO_3 (pH 8.2). (B) RP-HPLC oxidation profile of RgIA using 25% propan-2-ol in 0.1 M NH_4HCO_3 (pH 8.2). (C) Representative superimposed current traces evoked by 100 μM ACh without (control) and with 1 μM RgIA-ribbon and 10 nM RgIA-globular. (D) Concentration–response curves obtained for the inhibition of ACh-evoked peak current amplitudes by RgIA-globular (open circles) and RgIA-ribbon (open triangles). All data were pooled (n = 3–9 for each data point) and represent as arithmetic means ± S.E.M.

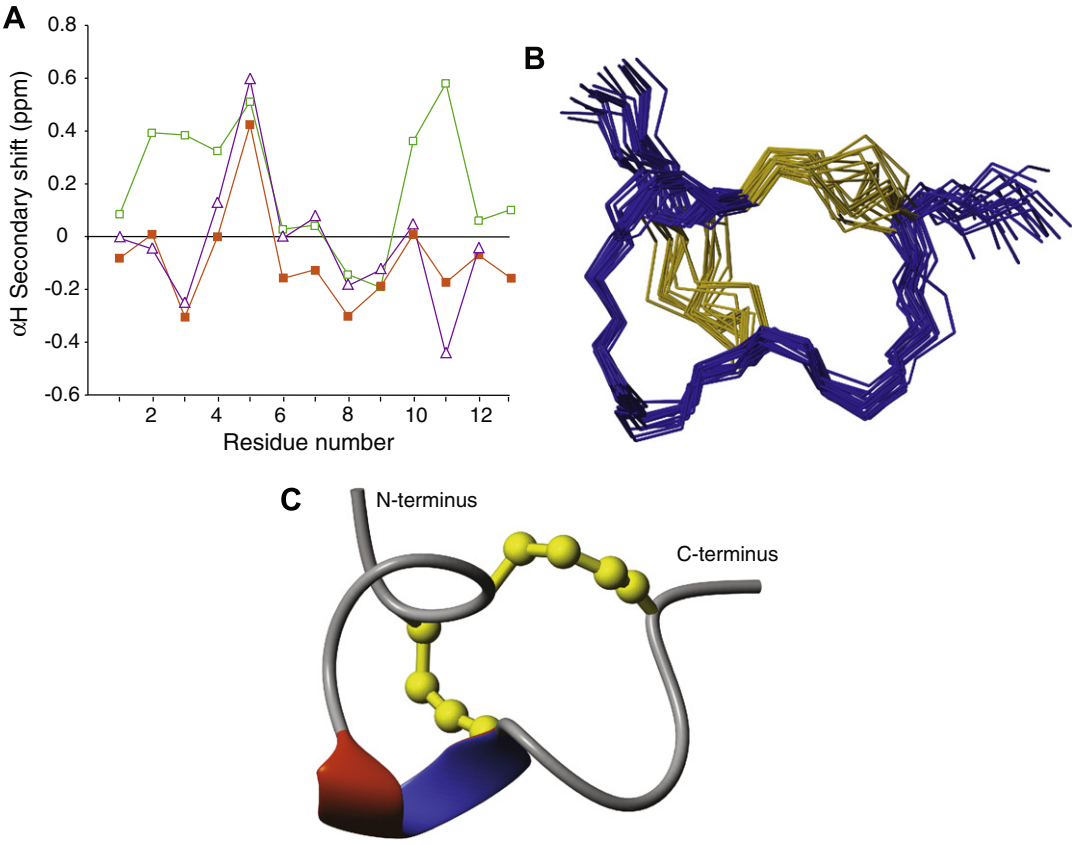

Fig. 3. NMR structure of RgIA. (A) Secondary shift analysis of the two isomers of RgIA compared to ImI [20]. Secondary shifts of the globular RgIA isomer (filled squares) are more comparable to those of ImI (open triangles) than those of the ribbon isomer (open squares). (B) NMR structure ensemble of RgIA. The peptide backbone is shown in blue and disulfide bonds are shown in yellow. (C) Mean 3D structure of RgIA showing the 3–10 helices.

O were included based on the analysis of slow exchange data and preliminary structures. The 20 lowest energy structures were chosen to represent the structure of RgIA and this ensemble is shown in Fig. 3B. A relatively well-defined structure was obtained, as shown by the RMSD over residues 2–11 of 0.46 ± 0.14 Å for the backbone atoms.

Analysis of the structures with PROMOTIF [17] identified a type I β-turn between residues 2 and 5, a 3_{10} helix between residues 5 and 9, and a type VIII β-turn between residues 9 and 12. The disulfide bond between Cys^2 and Cys^8 is characterized as a right-handed hook in approximately half the structures and the disulfide bond between residues Cys^3 and Cys^{12} does not have a preferred conformation. The mean structure of the ensemble is shown in Fig. 3C and the structural data have been deposited in the Biological Magnetic Resonance Data Bank (http://www.bmrb.wisc.edu/).

4. Discussion

RgIA is classified as a 4/3 α-conotoxin and the only other member of this sub-family for which a 3D structure has been determined is ImI [20–22]. The three published ImI structures show a very similar structure for loop 1 but the structures diverge in loop 2. There are also two X-ray crystal structures of ImI bound to the AChBP from *Aplysia*, which is a soluble homolog of the ligand binding domain of the nAChR [23,24]. Unlike RgIA, ImI is a selective inhibitor of the human α3β2 and α7 nAChR subtypes (IC_{50} = 41 and 595 nM, respectively) and is less potent at the α9α10 subtype (1.9 μM) [6,25]. Both ImI and RgIA share an identical loop 1 sequence but have different loop 2 sequences and it is proposed that this variation in the loop 2 sequences results in the differences in nAChR subtype selectivity of these two conotoxins [26].

Fig. 4 shows a comparison of the structure of RgIA with the crystal structure of ImI bound to the receptor where the residues from loop 1 have been overlaid. Loop 2 of RgIA matches quite closely to that of the bound ImI structure and suggests that similar binding modes are likely and that the differences in selectivity of the two conotoxins are due to the differences in the side chains of the three loop 2 residues. RgIA contains two arginines in loop 2 and one C-terminal arginine. This is reflected in the surface of the molecule (Fig. 4C), which is dominated by these positively charged residues and is in contrast to ImI which has a large hydrophobic patch comprizing Pro6 (from loop 1), Ala9 and Trp10 (from loop 2). Of the three loop 2 residues, the biggest difference between RgIA and ImI is at position 9, which is a large positively charged residue (Arg) in RgIA but a small hydrophobic residue (Ala) in ImI. In the crystal structure of ImI bound to the AChBP, Ala9 makes

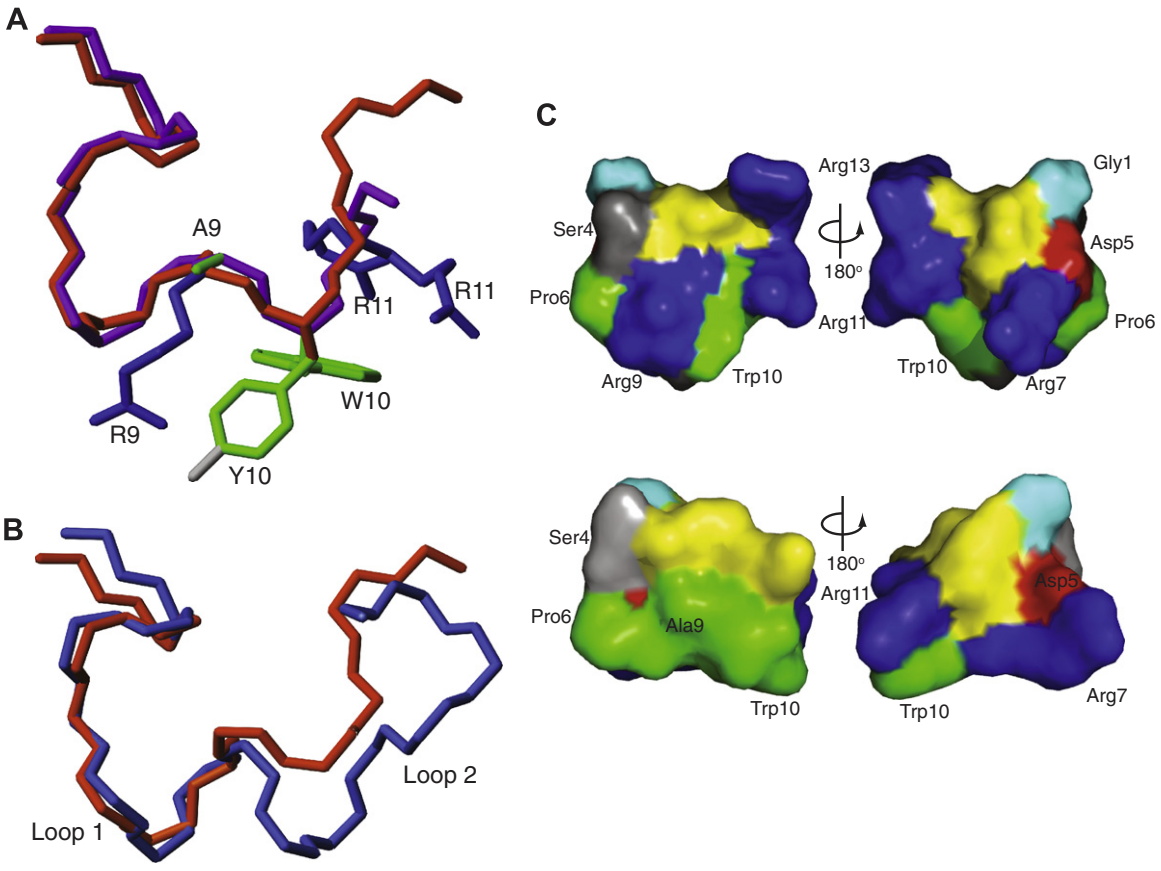

Fig. 4. Structural comparison of RgIA with ImI and Vc1.1 (A) Backbone superposition of RgIA (orange) and the AChBP bound ImI (purple, from PDB ID 2C9T) over loop 1. Sidechains of the loop 2 residues are shown with positively charged residues in blue, hydrophobic residues in green and the polar hydroxyl group of tyrosine in grey. (B) Backbone superposition of RgIA (orange) and Vc1.1 (blue, PDB ID 2h8s) overlayed over loop 1 (residues 2–8). (C) Molecular surfaces of RgIA (top) and ImI (bottom). Positive residues are blue; negative residues, red; hydrophobic residues, green, polar residues, grey; and glycine cyan.

contacts with Ile116 of the protein [24]. The α3β2 and α7 nAChR subtypes have a hydrophobic isoleucine or leucine, respectively, at position 116 but in the α9 and α10 nAChR subunits this hydrophobic residue is replaced by a negatively charged aspartic acid. It has been proposed that Arg9 in RgIA could form a salt bridge with the aspartic acid at position 116, which results in RgIA being selective for the α9α10 nAChR subtype [26]. The structure of RgIA is consistent with this proposal as the side chains of the residues at position 9 in both RgIA and bound ImI have a similar orientation (Fig. 4A) and therefore Arg9 in RgIA could potentially interact with Asp116 of the receptor.

The α-conotoxin Vc1.1, like RgIA, is selective for the α9α10 nAChR subtype and its loop 1 sequence is identical to that of RgIA. However, Vc1.1 is a member of the 4/7 subclass of α-conotoxins and has seven residues in loop 2 in contrast to RgIA, which has only three residues (Fig. 4B). Of the first three loop 2 residues of Vc1.1, only the tyrosine at position 10 is the same as RgIA. Importantly, the arginine at position 9 in RgIA that is believed to have a major role in the α9α10 selectivity of RgIA, by the formation of a salt bridge with the receptor, is an asparagine in Vc1.1 and therefore Vc1.1 cannot form this salt bridge. Vc1.1 clearly is capable of making receptor contacts that RgIA cannot make, simply due to its larger 2nd loop and these additional contacts are likely to result in the α9α10 selectivity of Vc1.1.

In conclusion, we have described the synthesis, folding and three-dimensional structure of RgIA, a selective antagonist of the α9α10 nAChR. This subtype has been proposed to play a role in the response to inflammation caused by nerve injury [9] and selective ligands may be valuable tools for elucidation of this pathway. Both RgIA and Vc1.1 have also been shown to be potent analgesics in rat models of neuropathic pain although the precise molecular target remains unknown [8–10]. These structural data on RgIA will facilitate further structure/function studies to understand the molecular mechanism of analgesia of these molecules via a range of approaches including peptide and receptor mutagenesis, molecular modelling studies and peptide engineering [27,28]. Recent studies on the α-conotoxin MII and the μ-conotoxin SIIIA, for example, have shown that structure guided engineering can be used to produce stabilized conotoxins via cyclization [27] or backbone prosthesis [28] that are potential drug leads.

Acknowledgements: We thank the Australian Research Council and the National Health and Medical Research Council for funding. D.J.C. is an ARC Professorial Fellow.

References

[1] Olivera, B.M. (2006) Conus peptides: biodiversity-based discovery and exogenomics. J. Biol. Chem. 281, 31173–31177.
[2] Miljanich, G.P. (2004) Ziconotide: neuronal calcium channel blocker for treating severe chronic pain. Curr. Med. Chem. 11, 3029–3040.
[3] Livett, B.G., Gayler, K.R. and Khalil, Z. (2004) Drugs from the sea: conopeptides as potential therapeutics. Curr. Med. Chem. 11, 1715–1723.
[4] Dutton, J.L. and Craik, D.J. (2001) alpha-Conotoxins: nicotinic acetylcholine receptor antagonists as pharmacological tools and potential drug leads. Curr. Med. Chem. 8, 327–344.
[5] Hu, S.H., Gehrmann, J., Alewood, P.F., Craik, D.J. and Martin, J.L. (1997) Crystal structure at 1.1 A resolution of alpha-conotoxin PnIB: comparison with alpha-conotoxins PnIA and GI. Biochemistry 36, 11323–11330.
[6] Ellison, M., Haberlandt, C., Gomez-Casati, M.E., Watkins, M., Elgoyhen, A.B., McIntosh, J.M. and Olivera, B.M. (2006) alpha-RgIA: A novel conotoxin that specifically and potently blocks the alpha9alpha10 nAChR. Biochemistry 45, 1511–1517.
[7] Sandall, D.W. et al. (2003) A novel alpha-conotoxin identified by gene sequencing is active in suppressing the vascular response to selective stimulation of sensory nerves in vivo. Biochemistry 42, 6904–6911.
[8] Satkunanathan, N., Livett, B., Gayler, K., Sandall, D., Down, J. and Khalil, Z. (2005) Alpha-conotoxin Vc1.1 alleviates neuropathic pain and accelerates functional recovery of injured neurones. Brain Res. 1059, 149–158.
[9] Vincler, M., Wittenauer, S., Parker, R., Ellison, M., Olivera, B.M. and McIntosh, J.M. (2006) Molecular mechanism for analgesia involving specific antagonism of alpha9alpha10 nicotinic acetylcholine receptors. Proc. Natl. Acad. Sci. USA 103, 17880–17884.
[10] Nevin, S.T., Clark, R.J., Klimis, H., Christie, M.J., Craik, D.J. and Adams, D.J. (2007) Are alpha9alpha10 nicotinic acetylcholine receptors a pain target for alpha-conotoxins? Mol. Pharmacol. 72, 1406–1410.
[11] Marx, U.C., Daly, N.L. and Craik, D.J. (2006) NMR of conotoxins: structural features and an analysis of chemical shifts of post-translationally modified amino acids. Magn. Reson. Chem. 44 Spec No, S41–S50.
[12] Schnölzer, M., Alewood, P., Jones, A., Alewood, D. and Kent, S.B.H. (1992) In situ neutralization in Boc-chemistry solid phase peptide synthesis. Int. J. Pept. Protein Res. 40, 180–193.
[13] Clark, R.J., Fischer, H., Nevin, S.T., Adams, D.J. and Craik, D.J. (2006) The synthesis, structural characterization, and receptor specificity of the alpha-conotoxin Vc1.1. J. Biol. Chem. 281, 23254–23263.
[14] Guntert, P., Mumenthaler, C. and Wüthrich, K. (1997) Torsion angle dynamics for NMR structure calculation with the new program DYANA. J. Mol. Biol. 273, 283–298.
[15] Brünger, A.T., Adams, P.D. and Rice, L.M. (1997) New applications of simulated annealing in X-ray crystallography and solution NMR. Structure 5, 325–336.
[16] Koradi, R., Billeter, M. and Wüthrich, K. (1996) MOLMOL: a program for display and analysis of macromolecular structures. J. Mol. Graph. 14 (51-5), 29–32.
[17] Hutchinson, E.G. and Thornton, J.M. (1996) PROMOTIF – A program to identify and analyze structural motifs in proteins. Protein Sci. 5, 212–220.
[18] Laskowski, R.A., Rullmannn, J.A., MacArthur, M.W., Kaptein, R. and Thornton, J.M. (1996) AQUA and PROCHECK-NMR: programs for checking the quality of protein structures solved by NMR. J. Biomol. NMR 8, 477–486.
[19] Nielsen, J.S., Bliczek, P. and Bulaj, G. (2004) Cosolvent-assisted oxidative folding of a bicyclic alpha-conotoxin ImI. J. Pept. Sci. 10, 249–256.
[20] Gehrmann, J., Daly, N.L., Alewood, P.F. and Craik, D.J. (1999) Solution structure of alpha-conotoxin ImI by 1H nuclear magnetic resonance. J. Med. Chem. 42, 2364–2372.
[21] Lamthanh, H., Jegou-Matheron, C., Servent, D., Menez, A. and Lancelin, J.M. (1999) Minimal conformation of the alpha-conotoxin ImI for the alpha7 neuronal nicotinic acetylcholine receptor recognition: correlated CD, NMR and binding studies. FEBS Lett. 454, 293–298.
[22] Rogers, J.P., Luginbuhl, P., Shen, G.S., McCabe, R.T., Stevens, R.C. and Wemmer, D.E. (1999) NMR solution structure of alpha-conotoxin ImI and comparison to other conotoxins specific for neuronal nicotinic acetylcholine receptors. Biochemistry 38, 3874–3882.
[23] Hansen, S.B., Sulzenbacher, G., Huxford, T., Marchot, P., Taylor, P. and Bourne, Y. (2005) Structures of Aplysia AChBP complexes with nicotinic agonists and antagonists reveal distinctive binding interfaces and conformations. Embo J. 24, 3635–3646.
[24] Ulens, C., Hogg, R.C., Celie, P.H., Bertrand, D., Tsetlin, V., Smit, A.B. and Sixma, T.K. (2006) Structural determinants of selective alpha-conotoxin binding to a nicotinic acetylcholine receptor homolog AChBP. Proc. Natl. Acad. Sci. USA 103, 3615–3620.
[25] Ellison, M., Gao, F., Wang, H.L., Sine, S.M., McIntosh, J.M. and Olivera, B.M. (2004) Alpha-conotoxins ImI and ImII target

distinct regions of the human alpha7 nicotinic acetylcholine receptor and distinguish human nicotinic receptor subtypes. Biochemistry 43, 16019–16026.
[26] Ellison, M. and Olivera, B.M. (2007) alpha4/3 Conotoxins: phylogenetic distribution, functional properties, and structure-function insights. Chem. Rec. 7, 341–353.
[27] Clark, R.J. et al. (2005) Engineering stable peptide toxins by means of backbone cyclization: stabilization of the alpha-conotoxin MII. Proc. Natl. Acad. Sci. USA 102, 13767–13772.
[28] Green, B.R. et al. (2007) Conotoxins containing nonnatural backbone spacers: cladistic-based design, chemical synthesis, and improved analgesic activity. Chem. Biol. 14, 399–407.